Krzysztof Duda and Tomasz P. Zieliński

The Polyphase Prony Method

Frequency and damping factor estimation, i.e., modal signal analysis, is a very important technical topic [1]–[11]. The Prony method [3] is widely used for frequency and damping estimation [4], [5] and is quite popular, although it suffers from poor noise immunity. In this article, we present a simple-to-implement trick, without any additional computational load, that improves the noise immunity of the Prony method. It is based on the proper selection of the sampling frequency [6]–[11], which seems to be overlooked in the signal processing community, or application of polyphase decomposition [12] to already acquired oversampled signals [10]. It is explained that having approximately four samples for the signal cycle is beneficial since if the sampling frequency is approximately four times the signal frequency, then approximate diagonalization of the 2×2 signal autocorrelation matrix occurs for a single damped sinusoid, which further results in its robust inversion in the linear prediction (LP) solution.

For signals sampled at higher rates, the LP equation should be separately built for each polyphase signal component, ensuring approximately four samples per cycle, and all equations should be combined and solved together. The method is further referred to as the *polyphase Prony method*. It is applied in [10] and [11] for a single damped and undamped sinusoid, respectively. Here, we present an intuitive derivation and explanation of the polyphase Prony method and its application for a single-frequency and a multifrequency damped signal.

Damped Sinusoidal Signal and Its Autocorrelation Sequence

We begin with a problem of estimation of an angular frequency ω_0 in radians and a damping factor of a single damped sinusoid x_n embedded in noise e_n:

$$\begin{aligned} s_n &= x_n + e_n \\ &= A_0 e^{-d_0 n}\cos(\omega_0 n + \phi_0) + e_n, \\ n &= 0, 1, 2, \ldots, N-1, \end{aligned} \tag{1}$$

where n denotes signal sample index, N is the number of samples, ϕ_0 is a phase in radians, $A_0 > 1$ is an amplitude, and $E_n = A_0 e^{-d_0 n}$ is an instantaneous amplitude or an envelope. The autocorrelation sequence estimate of a real-value finite-length sequence x_n is defined by

$$\begin{aligned} R_m &= \sum_{n=0}^{N-|m|-1} x_{n+|m|} x_n, \\ m &= -(N-1), \ldots, -1, 0, 1, \ldots, N-1. \end{aligned} \tag{2}$$

It is seen in (2) that R_m is symmetrical around shift $m = 0$. For a damped sinusoid x_n (1), R_m is given by the following closed-form formula:

$$\begin{aligned} R_m = \frac{A_0^2}{4} e^{-d_0|m|} \Bigg(& e^{-j(2\phi_0+\omega_0|m|)} \frac{1-e^{-2(j\omega_0+d_0)(N-|m|)}}{1-e^{-2(j\omega_0+d_0)}} \\ & + 2\cos(\omega_0|m|)\frac{1-e^{-2d_0(N-|m|)}}{1-e^{-2d_0}} \\ & + e^{j(2\phi_0+\omega_0|m|)} \frac{1-e^{2(j\omega_0-d_0)(N-|m|)}}{1-e^{2(j\omega_0-d_0)}} \Bigg). \end{aligned} \tag{3}$$

Figure 1 depicts autocorrelation sequence estimate (2) and (3) for an exemplary damped sinusoidal signal with $\omega_0 = \pi/8$ rad, i.e., sampled with 16 samples per cycle; $\omega_0 = \pi/2$ rad, i.e., sampled with four samples per cycle; and the R_1/R_0 ratio as a function of the signal phase for these two signals. In general, for $\omega_0 = \pi/2$ rad, R_1 is much smaller than R_0, what is crucial in

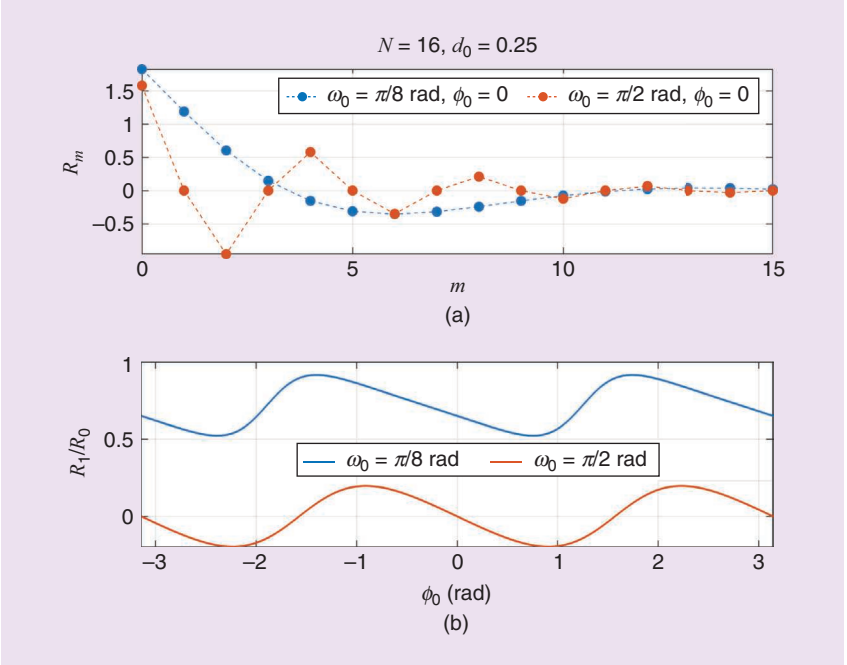

FIGURE 1. The autocorrelation sequence estimate (2) and (3) for (a) exemplary damped sinusoidal signal (1) for $m \geq 0$ and (b) the R_1/R_0 ratio as a function of the signal phase. Sampling with 16 samples per cycle ($\omega_0 = \pi/8$ rad) is shown in blue, and that with four samples per period ($\omega_0 = \pi/2$ rad) is presented in red.

Digital Object Identifier 10.1109/MSP.2022.3148712
Date of current version: 27 April 2022

further analysis, as it results in a close-to-diagonal matrix in least squares (LS) computations. It is observed from (3) that for $\omega_0 = \pi/2$ rad and $\phi_0 = 0$, we get $R_1 = 0$.

Diagonalization of Autocorrelation Matrix

For the damped sinusoid x_n in (1), the following LP equation holds:

$$\begin{aligned} x_n &= a_1 x_{n-1} + a_2 x_{n-2} \\ &= 2\cos(\omega_0) e^{-d_0} x_{n-1} - e^{-2d_0} x_{n-2}, \\ n &= 2, 3, \ldots, N-1, \end{aligned} \tag{4}$$

where $a_1 = 2\cos(\omega_0)e^{-d_0}$ and $a_2 = -e^{-2d_0}$, which is the basis for frequency and damping factor estimation in many methods. In this case, an overdetermined set of $N-2$ equations is built from signal samples, and next it is solved in the LS sense:

$$\begin{bmatrix} x_0 & x_1 \\ x_1 & x_2 \\ \vdots & \vdots \\ x_{N-3} & x_{N-2} \end{bmatrix} \begin{bmatrix} a_2 \\ a_1 \end{bmatrix} = \begin{bmatrix} x_2 \\ x_3 \\ \vdots \\ x_{N-1} \end{bmatrix},$$
$$\mathbf{X} \cdot \mathbf{a} = \mathbf{x}. \tag{5}$$

Knowing a_1 and a_2, we calculate ω_0 and d_0 from

$$\begin{aligned} d_0 &= -\frac{\ln(-a_2)}{2}, \\ \omega_o &= \cos^{-1}\left(\frac{a_1}{2e^{-d_0}}\right) \\ &= \cos^{-1}\left(\frac{a_1}{2\sqrt{-a_2}}\right). \end{aligned} \tag{6}$$

In straightforward LS computations, both sides of (5) are first left multiplied by matrix $\mathbf{X}^T$ (transposition) and then by matrix $(\mathbf{X}^T\mathbf{X})^{-1}$ (inversion), which results in

$$\mathbf{a} = (\mathbf{X}^T\mathbf{X})^{-1}\mathbf{X}^T \cdot \mathbf{x}. \tag{7}$$

We note that

$$\mathbf{X}^T\mathbf{X} = \begin{bmatrix} x_0 & x_1 & \cdots & x_{N-3} \\ x_1 & x_2 & \cdots & x_{N-2} \end{bmatrix} \begin{bmatrix} x_0 & x_1 \\ x_1 & x_2 \\ \vdots & \vdots \\ x_{N-3} & x_{N-2} \end{bmatrix}$$
$$= \begin{bmatrix} R_0^{(0)} & R_1 \\ R_1 & R_0^{(1)} \end{bmatrix} = \mathbf{R}, \tag{8}$$

where $R_0^{(0)}$, $R_0^{(1)}$, and R_1 are calculated from (2) for the following values of index n: R_1 for $n = 0, 1, 2, \ldots, N-2$; $R_0^{(0)}$ for $n = 0, 1, 2, \ldots, N-3$; and $R_0^{(1)}$ for $n = 1, 2, 3, \ldots, N-2$.

The inverse of a 2×2 symmetric matrix $\mathbf{R}$ is defined as

$$\mathbf{R}^{-1} = \frac{1}{\det(\mathbf{R})} \begin{bmatrix} R_0^{(1)} & -R_1 \\ -R_1 & R_0^{(0)} \end{bmatrix},$$
$$\det(\mathbf{R}) = R_0^{(0)} R_0^{(1)} - R_1^2. \tag{9}$$

If the elements of $\mathbf{R}$ are perturbed by a small amount [in general, we have to replace x_n in (8) with s_n defined in (1); i.e., the noise component e_n must be considered], then the consequent perturbation of $1/\det(\mathbf{R})$ in (9) is reduced when the value of $\det(\mathbf{R})$ is high. The values of $R_0^{(0)}$ and $R_0^{(1)}$ are both positive, and the highest value of $\det(\mathbf{R})$ is obtained for $R_1 = 0$; hence, $\mathbf{R}$ should be diagonal, and this occurs for $\omega_0 = \pi/2$ rad and $\phi_0 = 0$, as depicted in Figure 1.

Furthermore, other subtractions occurring during the multiplication of $\mathbf{R}^{-1} = (\mathbf{X}^T\mathbf{X})$ matrix in (7) amplify noise less when the absolute value of R_1 is small in comparison with $R_0^{(0)}$ and $R_0^{(1)}$. Therefore, the highest noise immunity of the solution is obtained for sampling with four samples per signal cycle. In general, the low value of the matrix condition number indicates the high noise immunity of the matrix inversion [13]. The matrix condition number is equal to the ratio of the maximum to the minimum matrix eigenvalue $\kappa(\mathbf{R}) = \lambda_{\max}/\lambda_{\min}$. The eigenvalues can be computed from the matrix characteristic polynomial, which, for the considered matrix $\mathbf{R}$, is given by the quadratic equation $(R_0^{(0)} - \lambda)(R_0^{(1)} - \lambda) - R_1 R_1 = 0$. Therefore,

$$\begin{aligned} \lambda_{\max} &= \frac{(R_0^{(0)} + R_0^{(1)}) + \Delta}{2}, \\ \lambda_{\min} &= \frac{(R_0^{(0)} + R_0^{(1)}) - \Delta}{2}, \\ \Delta &= \sqrt{(R_0^{(0)} - R_0^{(1)})^2 + 4R_1 R_1}, \end{aligned} \tag{10}$$

and condition number $\kappa(\mathbf{R}) = \lambda_{\max}/\lambda_{\min}$ reaches its minimum value, equal to

$$\kappa(\mathbf{R})_{\min} = \frac{R_0^{(0)}}{R_0^{(1)}} \tag{11}$$

for $R_1 = 0$. Thus, it is again confirmed that R_1 should be zero for the best noise robustness during the computation of (7).

Polyphase Signal Decomposition

In practice, sinusoidal signals are oversampled because, first, the variance of frequency and damping factor estimation decreases fast with the increase of the number of samples [14], assuming that the damping factor is not too high, and, second, a low-latency estimation is often desired by keeping the observation time as short as possible. For a higher number of samples per cycle, the LS solution should be applied to signal polyphase components, each with a frequency close to $\omega_0 = \pi/2$ rad, and not to the signal itself. The polyphase decomposition of a signal x_n into L subsequences $x_n^{(l)}$ is defined as [12]

$$x_n^{(l)} = x_{nL+l}, \quad l = 0, 1, \ldots, L-1 \tag{12}$$

and illustrated in Figure 2. Figure 2 presents one cycle of a damped sinusoid

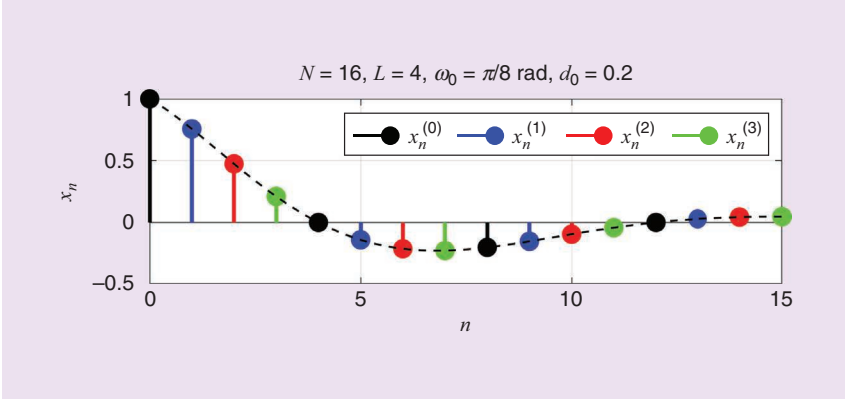

FIGURE 2. The exemplary polyphase decomposition of a damped sine, having 16 samples per cycle, into $L = 4$ components with four samples per cycle.

sampled with 16 samples per cycle; i.e., $\omega_0 = \pi/8$ rad. Straightforward application of the LS solution (6) to this signal has poor noise immunity. However, when the analyzed signal is first decomposed into $L = 4$ polyphase components with four samples per cycle, as shown in Figure 2, and than calculations are done, the obtained result is significantly improved. To avoid spectral aliases, the condition $\omega_o L < \pi$ must be fulfilled.

Therefore, to increase the noise immunity, (5) should be written in the following form:

$$\begin{bmatrix} \mathbf{X}^{(0)} \\ \vdots \\ \mathbf{X}^{(L-1)} \end{bmatrix} \begin{bmatrix} a_2^{(L)} \\ a_1^{(L)} \end{bmatrix} = \begin{bmatrix} \mathbf{x}^{(0)} \\ \vdots \\ \mathbf{x}^{(L-1)} \end{bmatrix}, \tag{13}$$

where $\mathbf{X}^{(l)}$ and $\mathbf{x}^{(l)}$ are matrixes and vectors defined as in (5) but built from polyphase signals $x_n^{(l)}$. For example, for the signal depicted in Figure 2 for $N = 16$ and $L = 4$, we have

$$\begin{bmatrix} x_0 & x_4 \\ x_4 & x_8 \\ x_1 & x_5 \\ x_5 & x_9 \\ x_2 & x_6 \\ x_6 & x_{10} \\ x_3 & x_7 \\ x_7 & x_{11} \end{bmatrix} \begin{bmatrix} a_2^{(4)} \\ a_1^{(4)} \end{bmatrix} = \begin{bmatrix} x_8 \\ x_{12} \\ x_9 \\ x_{13} \\ x_{10} \\ x_{14} \\ x_{11} \\ x_{15} \end{bmatrix} \quad \text{or}$$

$$\begin{bmatrix} x_0 & x_4 \\ x_1 & x_5 \\ x_2 & x_6 \\ x_3 & x_7 \\ x_4 & x_8 \\ x_5 & x_9 \\ x_6 & x_{10} \\ x_7 & x_{11} \end{bmatrix} \begin{bmatrix} a_2^{(4)} \\ a_1^{(4)} \end{bmatrix} = \begin{bmatrix} x_8 \\ x_9 \\ x_{10} \\ x_{11} \\ x_{12} \\ x_{13} \\ x_{14} \\ x_{15} \end{bmatrix}, \tag{14a and b}$$

with the colors in agreement with the polyphase signal components in Figure 2. Note that, e.g., submatrix $\mathbf{X}^{(0)}$ in (13) and (14a) has a 2×2 size and contains samples written in black. In (14b), rows of polyphase submatrices $\mathbf{X}^{(0)}, \ldots, \mathbf{X}^{(3)}$ are sorted in increasing order of sample indexes to stress that the number of equations is even lower than in the Prony method (5).

For the order of equations in (14b), the matrix $\mathbf{R}$ (8) is given by

$$\begin{aligned} \mathbf{R}^{(L)} &= \mathbf{X}^T \mathbf{X} \\ &= \begin{bmatrix} x_0 & x_1 & \cdots & x_{N-1-2L} \\ x_L & x_{L+1} & \cdots & x_{N-1-L} \end{bmatrix} \\ &\quad \times \begin{bmatrix} x_0 & x_L \\ x_1 & x_{L+1} \\ \vdots & \vdots \\ x_{N-1-2L} & x_{N-1-L} \end{bmatrix} \\ &= \begin{bmatrix} R_0^{(0)} & R_L \\ R_L & R_0^{(L)} \end{bmatrix}, \end{aligned} \tag{15}$$

where autocorrelation coefficients $R_0^{(0)}$, $R_0^{(L)}$, and R_L are calculated from (2), with n chosen similarly to the way it is in (8). It is observed in (14b) and (15) that the Lth-order polyphase signal decomposition effects the substitution of R_1 with R_L and $R_0^{(1)}$ with $R_0^{(L)}$ in autocorrelation matrix $\mathbf{R}$; thus, autocorrelation coefficients are computed with shift $m = L$ instead of $m = 1$, which should be exploited in implementation. In the Prony and polyphase Prony methods, all signal samples are used. However, in the Prony method (5), the number of equations is equal to $N - 2$ (14 in our example), while in the polyphase Prony method (14), it is lower and equals $N - 2L$ (eight in our example). Finally, the estimated damping factor and frequency values calculated by (6) must be divided by L:

$$d_0 = \frac{d_0^{(L)}}{L}, \quad \omega_0 = \frac{\omega_0^{(L)}}{L}. \tag{16}$$

This division by L leads to a reduction of the overall estimation error, as explained further.

The Prony method is widely used for frequency and damping estimation and is quite popular, although it suffers from poor noise immunity.

Multifrequency Signal

A multifrequency signal is a sum of damped sinusoids of the form (1), and there are two additional components in difference equation (4) for each real-value sinusoidal component; i.e.,

$$\begin{aligned} x_n &= \sum_{k=0}^{K} A_k e^{-d_k n} \cos(\omega_k n + \phi_k) \\ &= a_1 x_{n-1} + a_2 x_{n-2} + \cdots \\ &\quad + a_{2K-1} x_{n-(2K-1)} + a_{2K} x_{n-2K}, \end{aligned} \tag{17}$$

where K denotes the number of components. After building a set of equations similar to (5) and solving it in regard to a_k, the frequency and damping factor are computed by (16) using d_k and ω_k obtained from the roots $r_k = e^{-d_k \pm j\omega_k}$ of the polynomial $p(x) = 1 - a_1 z^{-1} - a_2 z^{-2} - \cdots - a_{2K} z^{-2K}$ resulting from (17). By Euler's formula, every real-value sinusoidal component in (17) is a sum of two complex-value signals, i.e., $\cos(\omega_k n + \varphi_k) = (e^{j(\omega_k n + \varphi_k)} + e^{-j(\omega_k n + \varphi_k)})/2$, and for frequency and damping factor computations, the roots r_k with positive frequencies are selected. For a complex-value signal, as, e.g., in nuclear magnetic resonance spectroscopy, the Prony method can be used to resolve all, i.e., positive and negative, frequency components.

Details of the Prony method can be found, e.g., in [3]. For the multifrequency signal (17), the autocorrelation matrix $\mathbf{R}$ [analogous to (8)] has size $2K \times 2K$. In this case, the sampling frequency can be adjusted to obtain low condition number $\kappa(\mathbf{R})$ based on initial analysis of signal components, which improves the noise immunity of signal reconstruction from estimated parameters [9]. In [9], a damped multifrequency signal with components $\{500, 1{,}100, 1{,}400\}$ Hz is reported to be optimally sampled with a frequency of 3,800 Hz, which results in $\{7.6, 3.45, 2.71\}$ samples per cycle of each component, respectively. In this example, a mean frequency 1,000 Hz contains 3.8 samples per cycle, and the mean number of samples per signal's component cycle is 4.59. In general, it is not possible to obtain a very small frequency and damping estimation error simultaneously for all signal components for arbitrary multifrequency signal in the Prony and polyphase Prony methods. However, for oversampled signals, the polyphase Prony method outperforms the Prony method, as further illustrated in Example 2.

Example 1: Optimal Sampling of a Single Damped Sinusoid

It is assumed that the analyzed continuous-time signal is sampled in a fixed-time observation interval with different sampling frequencies, and the number of acquired cycles and the envelope are the same in each discrete-time representation (1). For this reason, in the simulations, we refer to the number of cycles in the observation interval k_0, defined as

$$\omega_0 = \frac{2\pi}{N} k_0, \tag{18}$$

and not to the frequency ω_0. For integer values, k_0 is the number of the discrete Fourier transform (DFT) frequency bin. We also relate the damping factor d_0 to the number of samples:

$$D = d_0 N. \tag{19}$$

Thanks to (19), the shape of the envelope is preserved for an arbitrary number of samples N. The ratio of envelope values at the end and the beginning of the signal is $E_N/E_0 = e^{-D}$, so it is easy to estimate the strength of the damping factor independently from the number of samples N. Figure 3 illustrates the performance of the polyphase Prony method for a signal containing $N = 64$ samples embedded in 40-dB additive zero-mean white Gaussian noise (AWGN). The frequency is swept in the range from 0 to $\pi/2$ rad, which corresponds to k_0 changed from 0 to $N/4 = 16$. For each frequency, the phase is a random variable with uniform distribution. Figure 3 presents the root-mean-square error (RMSE) of the frequency estimation. The results in Figure 3 are also referred to the *Cramér–Rao Lower Bound* (*CRLB*) [14], plotted in a black dotted line. The results for the damping factor are not presented, as they look similar.

The curves are plotted for different numbers of polyphase components $L = 1, 2, \ldots, 16$. For $L = 1$, there is no polyphase decomposition; thus, it is the Prony method. It is observed that the minimum RMSE for $L = 1$ occurs for $k_0 = 16$; i.e., $\omega_0 = \pi/2$ rad, as expected. For $L > 1$, the measurement range narrows due to the $\omega_o L < \pi$ condition. For $L = 2$, the maximum allowed signal frequency is $\pi/2$ rad, and the minimum RMSE is obtained for $\omega_0 = \pi/4$ rad; i.e., $k_0 = 8$. It is observed that along with the increase of L, the frequency estimation is getting closer to the optimal estimator, i.e., to the CRLB. We also note that the curves in Figure 3(a) are quite flat in the neighborhood of the minimum value, which is advantageous because it broadens the measurement range of the estimator. The minimum RMSE, marked by black dots in Figure 3, decreases with the increase of L, due to the division by L in (16); i.e., initially, ω_0 is estimated with some error, but next, this estimate is divided by L and so is the estimation error. From the performed simulation, it is observed that the RMSE decreases roughly no faster than $1/\sqrt{L}$ because the noise influence is stronger for a single polyphase component than for the Prony method, as there are fewer samples in each polyphase component [11].

In conclusion, the noise immunity of the polyphase Prony method is increased by two means: 1) the selection of the optimal sampling frequency of the polyphase components, i.e., four samples per cycle, and 2) the division of the initial estimate by the number of polyphase components. The improvement over the RMSE offered by polyphase decomposition is shown in Figure 3(a) with a black solid line, where black dots mark RMSE values at frequencies $\pi/(2L)$ rad, i.e., for the optimal four

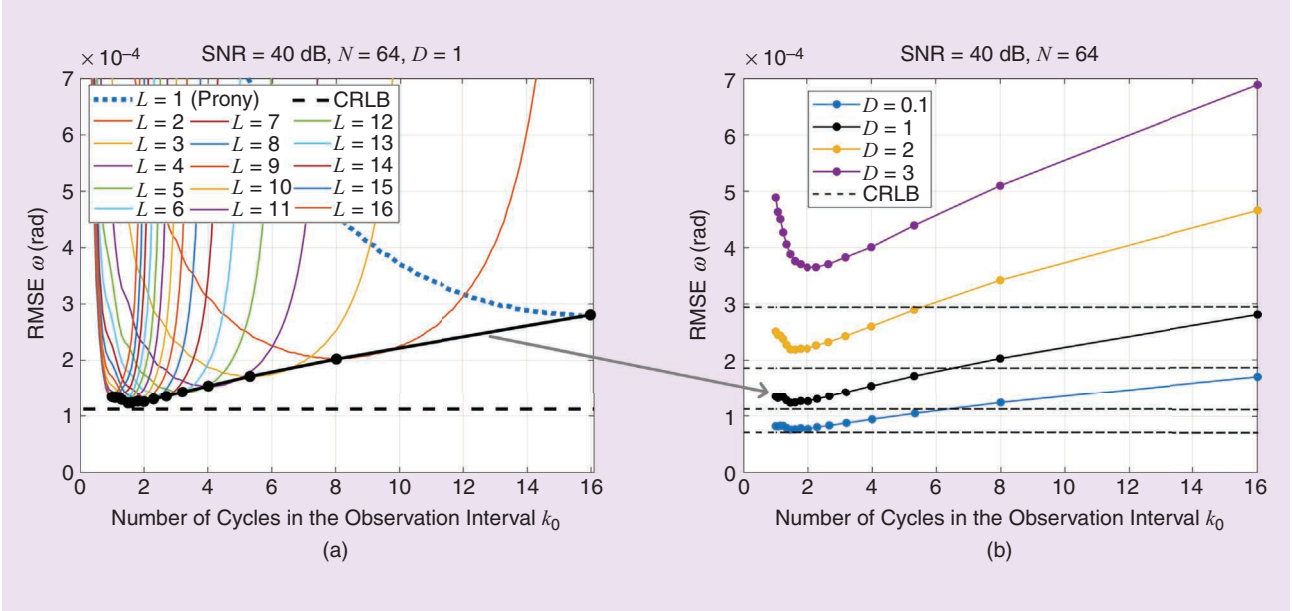

FIGURE 3. (a) The root-mean-square error (RMSE) of frequency estimation: $N = 64$, $D = 1$, and the signal-to-noise ratio (SNR) = 40 dB; black dots mark RMSE values at frequencies $\pi/(2L)$ rad, i.e., for four samples per cycle. (b) The RMSE at frequencies $\pi/(2L)$ rad for different damping factors D. Only results obtained for L ensuring four samples per cycle are shown [the black lines in (a) and (b) $(D = 1)$ are the same, as indicated by the gray arrow). CRLB: Cramér–Rao Lower Bound.

samples per cycle. The smallest RMSE for the Prony method, in Figure 3(a), at $k_0 = 16$ is around 2.5 times higher than the CRLB, whereas for the polyphase Prony method, at $k_0 = 2$ the RMSE is only around 1.11 times higher than the CRLB. We also note that for $k_0 = 2$, the RMSE for the Prony method is about 16 times higher than the CRLB, and it is out of the axis range in Figure 3. Figure 3(b) depicts the RMSE at frequencies $\pi/(2L)$ rad for different values of damping factor D. In this case, the experiment performed and reported in Figure 3(a) for $D = 1$ was repeated for different values of $D = \{0.1, 1, 2, 3\}$, but only results obtained for L ensuring four samples per cycle are plotted [note that the black curve for $D = 1$ is the same in Figure 3(a) and (b)].

It is observed that when the damping increases, the RMSE also increases, as expected, because the autocorrelation coefficient $R_0^{(1)}$ decreases faster than $R_0^{(0)}$, which causes the increase of the condition number $\kappa(\mathbf{R})$ (11). The RMSE curve retains its shape, but it is shifted up with stronger damping. Results (not reported here) obtained for a higher number of samples N lead to similar conclusions about the sampling frequency. As a rule of thumb, the optimal signal sampling is obtained in the neighborhood of $k_0 = 2$. For example, for a 50-Hz sinusoid and $N = 64$ samples for $k_0 = 2$, there are 32 samples in one cycle, and the sampling frequency $50 \cdot 32 = 1{,}600$ Hz should be chosen along with polyphase factor $L = 32/4 = 8$. This setup will result in a small RMSE in LP-based frequency and damping factor estimation.

Example 2: Multifrequency Signal

In this example, we estimate the frequencies and damping factors of all 10 components in the test signal from the signal embedded in 40-dB AWGN. The signal has $N = 512$ samples. The components consist of $k_0 = \{10.24, 9.76, 8.79, 7.84, 7.26, 6.84, 6.01, 5.52, 5.03, 4.37\}$ cycles, which approximately corresponds to frequencies in radians $\omega_0 = \{0.126, 0.12, 0.108, 0.096, 0.089, 0.084, 0.074, 0.068, 0.062, 0.054\}$, and the damping factors of the components are $D = \{1.13, 1.07, 1.02, 0.95, 0.85, 1.15, 1.05, 1, 0.95, 0.85\}$. We note that this test signal cannot be resolved by the DFT-based methods because neighboring frequencies are separated by less than $2\pi/N \approx 0.012$ rad, i.e., by less than the DFT frequency resolution. Figure 4(a) depicts all components of the test signal; the signal itself, i.e., the sum of the components; and its magnitude spectrum. In simulation, the phases of all 10 components were chosen at random in each realization. The RMSE of every frequency component estimation from 10^5 realizations as a function of L is depicted in Figure 4(b).

For signals sampled at higher rates, the LP equation should be separately built for each polyphase signal component, ensuring approximately four samples per cycle.

The highest-frequency component in the test signal contains 10.24 oscillations; thus, the integer L for this component must be lower than $512/10.24/2 = 25$ (to prevent frequency aliasing, the signal must have more than two samples per cycle). Figure 4(b) shows that it is beneficial to apply $L > 1$, i.e., to use the polyphase Prony method instead of the Prony method $(L = 1)$. For the considered signal, the RMSE decreases with L for high frequencies [dashed lines in Figure 4(b)]. For the signal with the smallest frequency, the best L equals 8. In general, the selection of the optimum L value, with respect to the RMSE, is not as obvious for a multifrequency signal as it is for a single-frequency signal in Example 1. For a multifrequency signal, sinusoidal

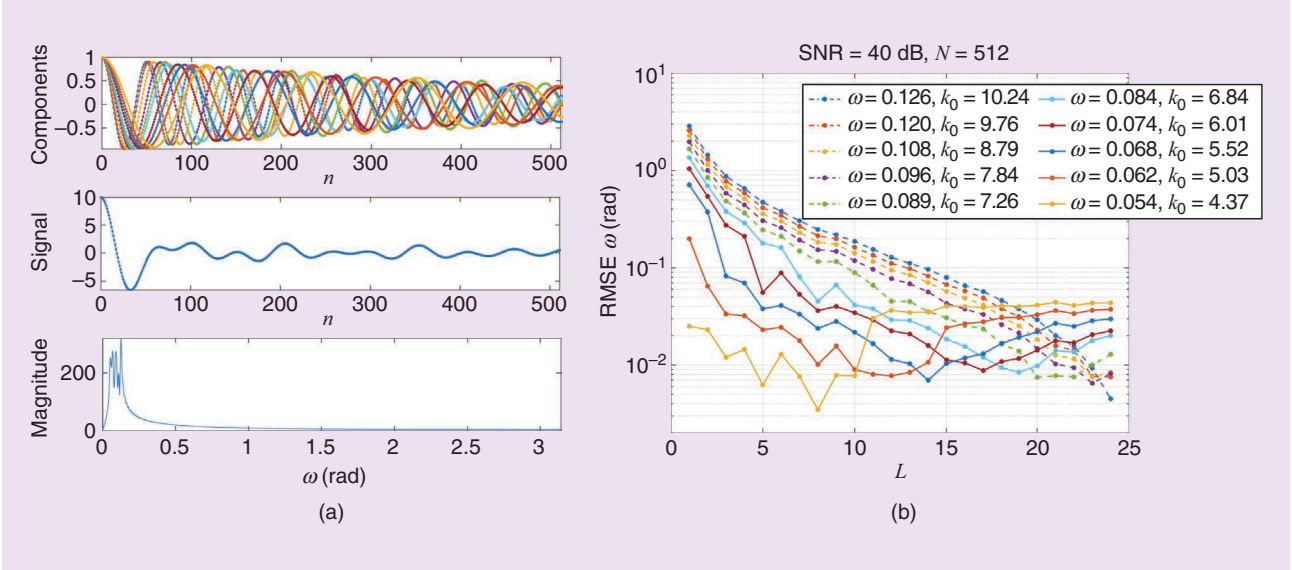

FIGURE 4. The multifrequency test signal (a) without noise and with zero phase, and (b) the RMSE of the frequency estimation of each frequency component for the Prony method $L = 1$ and the polyphase Prony method $L > 1$ for a signal embedded in SNR = 40-dB noise.

components should be concentrated in the narrow frequency band, and L should be chosen so as to obtain four samples per signal cycle for the highest-frequency component or four samples per signal cycle for the middle-frequency component, provided that the highest-frequency component is still sampled more than two samples per cycle. If frequency components occupy the whole spectrum, then the polyphase Prony method is not applicable in a straightforward way.

The application of the polyphase Prony method improves noise immunity without any extra computational costs.

Conclusions

We have shown that by selecting the right signal sampling frequency or applying polyphase signal decomposition, the noise immunity of frequency and damping factor estimation can be significantly increased in the Prony method and that the CRLB is almost reached for a single sinusoid. The application of the polyphase Prony method improves noise immunity without any extra computational costs. In fact, it requires slightly fewer computations than the Prony method. For a multifrequency signal, the polyphase trick generally still holds; however, its mathematical explanation and quasi-optimal adjustment are much more difficult [9]. For increased noise immunity, a high number of samples is required; thus, signal oversampling is recommended.

From our experience, the polyphase Prony method is especially useful for the analysis of a single sinusoid since, in this case, it can be configured for optimal performance even for a small number of signal cycles; see [11] for the undamped sine case. For a multifrequency signal, the polyphase Prony method performs better than the Prony method itself, but it is not optimal for noise suppression, and other techniques, such as, e.g., the Steiglitz–McBride approach [5], should be considered. The Steiglitz–McBride method is an iterative algorithm that repeatedly applies an infinite impulse response filter and LP solution. It closely tracks the CRLB; thus, no improvement can be made by applying the presented polyphase trick to this method. The polyphase Prony method can reach the performance of the Steiglitz–McBride method for a single sinusoid with significantly lower computational complexity; e.g., in [11], it is shown that, for a single undamped sinusoid, the polyphase Prony method executes in MATLAB approximately 30 times faster than the Steiglitz–McBride method.

We also note that the Prony method applied to a downsampled version of the original signal, obtained by replacing each consecutive block of L original signal samples by their average value or, equivalently, by averaging all polyphase signal components, has a higher RMSE than the proposed polyphase Prony approach.

Acknowledgment

We would like to thank Prof. Bogdan Matuszewski, University of Central Lancashire, Preston, U.K., for a fruitful discussion about the final form of the article.

Authors

Krzysztof Duda (kduda@agh.edu.pl) received his Ph.D. degree in electronics from AGH University of Science and Technology (AGH-UST) in 2002. Since 2019, he has been a professor in the Department of Measurement and Electronics, AGH-UST, Kraków, 30059, Poland. His research interests include the development and applications of digital signal processing and analysis.

Tomasz P. Zieliński (tzielin@agh.edu.pl) received his Ph.D. degree in electrical engineering from the Bulgarian Academy of Sciences, Sofia, Bulgaria, in 1988. He has been a full professor in the Department of Telecommunications, AGH University of Science and Technology, Kraków, 30059, Poland, since 2006. His research interests include advanced digital signal processing in telecommunication and biomedical systems, particularly time–frequency signal analysis. In 2021, he authored the textbook *Starting Digital Signal Processing in Telecommunication Engineering. A Laboratory-Based Course* with many tips and tricks.

References

[1] J. C. Visschers, E. Wilson, T. Conneely, A. Mudrov, and L. Bougas, "Rapid parameter determination of discrete damped sinusoidal oscillations," *Opt. Exp.*, vol. 29, no. 5, pp. 6863–6878, Mar. 2021, doi: 10.1364/OE.411972.

[2] K. E. Jacobson, J. F. Kiviaho, G. J. Kennedy, and M. J. Smith, "Evaluation of time-domain damping identification methods for flutter-constrained optimization," *J. Fluids Struct.*, vol. 87, pp. 174–188, May 2019, doi: 10.1016/j.jfluidstructs.2019.03.011.

[3] S. M. Kay and S. L. Marple, "Spectrum analysis—A modern perspective," *Proc. IEEE*, vol. 69, no. 11, pp. 1380–1419, 1981, doi: 10.1109/PROC.1981.12184.

[4] H. C. So, K. W. Chan, Y. T. Chan, and K. C. Ho, "Linear prediction approach for efficient frequency estimation of multiple real sinusoids: Algorithms and analyses," *IEEE Trans. Signal Process.*, vol. 53, no. 7, pp. 2290–2305, Jul. 2005, doi: 10.1109/TSP.2005.849154.

[5] T. P. Zieliński and K. Duda, "Frequency and damping estimation methods - An overview," *Metrol. Meas. Syst.*, vol. 18, no. 4, pp. 505–528, 2011, doi: 10.2478/v10178-011-0051-y.

[6] R. W. Kulp, "An optimum sampling procedure for use with the Prony method," *IEEE Trans. Electromagn. Compat.*, vol. EMC-23, no. 2, pp. 67–71, May 1981, doi: 10.1109/TEMC.1981.303896.

[7] A. Agneni, "Modal parameter estimates from autocorrelation functions of highly noisy impulse responses," *Int. J. Analytical Exp. Modal Anal.*, vol. 7, no. 4, pp. 285–297, Oct. 1992.

[8] J.-H. Lee and H.-T. Kim, "Selecting sampling interval of transient response for the improved Prony method," *IEEE Trans. Antennas Propag.*, vol. 51, no. 1, pp. 74–77, Jan. 2003, doi: 10.1109/TAP.2003.808551.

[9] O. Y. Bushuev, and O. L. Ibryaeva, "Choosing an optimal sampling rate to improve the performance of signal analysis by Prony's method," in *Proc. 2012 35th Int. Conf. Telecommun. Signal Process. (TSP)*, Prague, pp. 634–638, doi: 10.1109/TSP.2012.6256374.

[10] J. Yuan and M. Torlak, "Modeling and estimation of transient carrier frequency offset in wireless transceivers," *IEEE Trans. Wireless Commun.*, vol. 13, no. 7, pp. 4038–4049, Jul. 2014, doi: 10.1109/TWC.2014.2328345.

[11] K. Duda and T. P. Zielinski, "Fast one-cycle frequency estimation of a single sinusoid in noise using downsampled linear prediction model," *Metrol. Meas. Syst.*, vol. 28, no. 4, pp. 661–672, 2021, doi: 10.24425/mms.2021.137701.

[12] A. V. Oppenheim, R. W. Schafer, and J. R. Buck, *Discrete-Time Signal Processing (Multirate Signal Processing)*, 2nd ed. Upper Saddle River, NJ, USA: Prentice-Hall, 1999, ch. 4.7, pp. 179–184.

[13] T. K. Moon and W. C. Stirling, *Mathematical Methods and Algorithms for Signal Processing (Matrix Condition Number)*. Upper Saddle River, NJ, USA: Prentice-Hall, 1999, ch. 4.10, pp. 253–258.

[14] Y.-X. Yao and S. M. Pandit, "Cramér-Rao lower bounds for a damped sinusoidal process," *IEEE Trans. Signal Process.*, vol. 43, no. 4, pp. 878–885, Apr. 1995, doi: 10.1109/78.376840.

SP